Unsymmetrically ligated dioxobridged Mn(III, IV) complexes – synthesis and spectral studies

G SWARNABALA and M V RAJASEKHARAN*

School of Chemistry, University of Hyderabad, Hyderabad 500 134, India

Abstract. The mixed valence Mn(III, IV) complexes, $[Mn_2O_2L_4]X_3$ with $L = 2,2$-bipyridine or 1,10-phenanthroline and $X = ClO_4^-$ or PF_6^- undergo partial ligand displacement reactions giving rise to the new compounds $[Mn_2O_2L_3A_2]X_3$ with $A = N,N$-dimethylformamide or pyridine. The substitution is believed to take place at the labile d^4, Mn(III) centre. The substituted complexes have more deeply trapped valencies based on their electronic spectral characteristics. The EPR spectra are found to be essentially unaffected by ligand substitutions. Computer simulations of frozen solutions as well as polycrystalline spectra of the PF_6^- salts showing hyperfine splittings are presented. All the complexes evolve oxygen from water when present as a solid phase in contact with an aqueous solution containing Ce^{4+} ions. The oxygen-evolving solution is found to contain MnO_4^- ions.

Keywords. Mixed valency; Mn(III, IV) complexes; EPR; oxygen evolution.

1. Introduction

Mixed valence manganese centres are known to play a key role in the evolution of oxygen by water oxidation in photosystem-II (Dismukes and Siderer 1981; Kambara and Govindjee 1985; Paula and Brudvig 1985; Biggins 1987; Mulay and Padhye 1987). Details regarding the structure of the Mn-site and the reaction mechanism are not clear. Mixed valence compounds containing polypyridyl and related ligands have been proposed as models. Following the first preparation of $[Mn_2O_2(bpy)_4](S_2O_8)_{1.5}$ by Nyholm and Turco (1960), several reports have dealt with the structure and magnetic properties of Mn(III, IV) complexes of 2,2'-bipyridine (bpy) and 1,10-phenanthroline (phen) (Plaksin et al 1972; Cooper and Calvin 1977; Cooper et al 1978; Inoue 1978; Morrison and Sawyer 1978; Ramaraj et al 1986; Stebler et al 1986). The observation of multiline EPR spectra from the S_2 state of the water oxidation centre by Dismukes and Siderer (1981), which is very similar to the spectra of $[Mn_2O_2(bpy)_4]^{3+}$ has generated considerable interest in these systems as biomimetic models.

In the present paper we address the following questions: (i) Can the substitutional lability expected of the Mn(III) (d^4) site as opposed to the inertness of the Mn(IV) (d^3) site be exploited to prepare unsymmetrically ligated dinuclear complexes? (ii) Will crystallisation with large counter-ions like PF_6^- give rise to magnetically dilute mixed-

---

valence compounds? (iii) What are the factors which determine the EPR parameters of exchange-coupled dinuclear Mn(III, IV) complexes and what is the influence of the environment (ligands and host matrices) on these factors? Partial substitution by ligands like N, N-dimethylformamide (DMF) and pyridine (py) on the symmetrical dinuclear complexes and the analytical and spectral characterisation of the resultant products will be discussed. Solid state EPR spectra of the PF_6^- salts showing hyperfine splittings and simulation of polycrystalline and frozen solution spectra, as well as preliminary results on the water oxidation studies are also presented.

2. Experimental

2.1 *Solvents and reagents*

All the organic solvents were purified by the following standard procedures (Furniss *et al* 1978). N, N-Dimethylformamide was distilled under dry nitrogen and stored over type 4A molecular sieves. 2, 2'-Bipyridine (bpy) and 1, 10-phenanthroline (phen) were purchased from Aldrich Chemicals. 4, 4'-Dimethyl-2, 2'-bipyridine (4, 4'-dmbp) and 5, 5'-dimethyl-2, 2'-bipyridine (5, 5'-dmbp) were prepared from γ-picoline and β-picoline respectively by coupling over W7-J Raney nickel (Sasse and Whittle 1961).

2.2 *Preparation of Mn(III, IV) complexes*

$[Mn_2O_2L_4]X_3$, L = bpy, phen, 4, 4'-dmbp, 5, 5'-dmbp, $X = ClO_4^-$, BF_4^-, PF_6^- were prepared by adapting the previously reported procedure for $[Mn_2O_2(bpy)_4](ClO_4)_3$ (Cooper and Calvin 1977).

2.3 *DMF substitution*

$Mn_2O_2(phen)_4(PF_6)_3$ was dissolved in the minimum amount of DMF to give a green-coloured solution. This on standing for several days in a dessicator changes colour to red. The change in colour was monitored by optical spectral measurements. The solution was then precipitated by using dry ether. The red precipitate was washed several times with dry ether and dried in vacuum. Analysis, C = 39·95, H = 2·88, N = 8·80, phen (by spectrophotometry) = 43%. $Mn_2O_2(phen)_3(DMF)_2(PF_6)_3$ requires, C = 39·92, H = 3·03, N = 8·87, phen = 42·79%. This product was found to be moisture-sensitive, turning to pink after standing for several weeks. The analogous procedure for the bpy complex resulted in an impure gummy material.

2.4 *Pyridine substitution*

$[Mn_2O_2L_4](ClO_4)_3$, L = bpy or phen was dissolved in pyridine and filtered. The clear green solution was left for crystallisation by slow evaporation. The green crystalline material which deposited after a few days was collected, washed with small amounts of pyridine and dried. Analysis, for the phen complex, C = 48·73, H = 2·97, N = 10·10%, $Mn_2O_2(phen)_3(py)_2(ClO_4)_3$ requires C = 48·51, H = 2·98, N = 9·84%. Analysis for the bpy complex, C = 44·48 H = 3·02, N = 9·31%, $Mn_2O_2(bpy)_3(py)_2(ClO_4)_3$ requires C = 45·03, H = 3·21, N = 10·50%.

2.5 *Physical measurements*

Elemental (C, H, N) analysis, IR spectra, and UV-visible spectra were obtained using Perkin-Elmer instruments, viz. the 240 C analyser, IR 1310 or 297, and LAMBDA-3 spectrophotometer, respectively. EPR spectra were recorded on a JEOL FE 3X spectrometer equipped with a variable temperature cryostat. DPPH was used for calibration ($g = 2 \cdot 0036$).

2.6 *Computer simulation of EPR spectra*

A previously described computer program (Rajasekharan and Manoharan 1981) was modified to include ligand hyperfine interactions in first order. For simulating the hyperfine interaction in the dinuclear complexes, one Mn nucleus was taken as the central atom and the other Mn nucleus was treated as 'ligand'. The g- and hyperfine tensors were assumed to be axial with coincident principal axes. The calculations were carried out on a WIPRO IBM compatible personal computer.

3. Results and discussion

3.1 *Substitution reactions*

The $[Mn_2O_2L_4]^{3+}$ salts (L = bpy, phen) dissolve readily in DMF and pyridine. The DMF solutions are reddish brown while in pyridine the green colour is retained. All solutions, however, contain dinuclear species as evidenced by the multiline EPR spectra (*vide supra*). Partially substituted complexes could be precipitated from these solutions which analyse as $[Mn_2O_2L_3A_2]^{3+}$ salts (L = phen, A = DMF, py, and L = bpy, A = py). The IR spectra of the substituted complexes have features corresponding to DMF and py in addition to those of the parent complexes. The DMF complex is much more reactive being instantly reduced by water giving a pale yellow solution. Attempts to obtain single crystals were futile in this case. The crystal structure determination of the analogous β-picoline complex is under way.

Mixed ligand complexes were also obtained when the phen complex was crystallised from bpy/bpyH$^+$ buffer and vice versa. These compounds are tentatively formulated as $[Mn_2O_2(phen)_3 (bpy)]^{3+}$ and $[Mn_2O_2(bpy)_3phen]^{3+}$ salts. They differ from the parent complexes in their spectral characterstics.

3.2 *Electronic and EPR spectra*

The true symmetry at each of the Mn-sites in these dinuclear species is not higher than C_{2v}. A large distortion is expected for the ^5E_g ground state derived from the $t_{2g}{}^3e_g$ configuration of the Mn^{3+} site. This will yield a transition in the near IR or visible region. Other spin-allowed transitions localised on Mn^{3+} and Mn^{4+} centres are expected at higher energy, some of which may be masked by charge transfer and intra-ligand transitions. The electronic spectra of the phen and bpy complexes in aqueous buffer (pH 4·5) were first reported by Cooper and Calvin (1977). Absorption maxima are seen at 19·0, 18·0 and 14·6 kK along with a broad shoulder around 12·0 kK. The broad band was assigned to the intervalence transfer absorption (IVTA). We find that for both complexes the IVTA band shifts to 13·6 kK in acetonitrile solution (figure 1a).
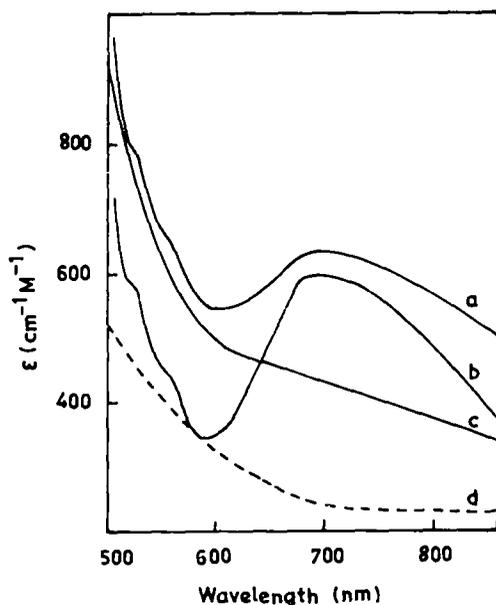
Figure 1. Visible absorption spectra of (a) $Mn_2O_2(phen)_4(PF_6)_3$ in acetonitrile, (b) $Mn_2O_2(phen)_3(bpy)(ClO_4)_3$ in acetonitrile, (c) $Mn_2O_2(phen)_4(PF_6)_3$ in DMF, and (d) $Mn_2O_2(phen)_4(ClO_4)_3$ in pyridine.

The other band positions are unaffected. In DMF and pyridine, the visible band is almost completely swamped by the tail of the UV absorption (figures 1c and d). Since within the model of Hush (1967) only changes in intensity are expected for the IVTA band as a function of solvent, the above observations show that even a relatively inert solvent like acetonitrile is able to chemically perturb the dimeric ion in solution. In the case of DMF and py, substitution takes place which considerably inhibits the mixed-valent delocalisation as implied by the low intensity of the IVTA band. Since the major contribution to the low energy band arises from the very broad IVTA, the substituted complexes have relatively featureless optical absorption spectra. In the case of $Mn_2O_2(bpy)_3$ phen$(ClO_4)_3$ and $Mn_2O_2(phen)_3$bpy$(ClO_4)_3$ in acetonitrile there is an unexplained sharpening of the visible band without change in its position (figure 1b).

EPR spectra of polycrystalline samples show broad (dipolar or exchange averaged) lines. Partial resolution of the hyperfine splitting is seen in a few cases (figure 2). Frozen solutions give much better resolution and the spectra are almost identical for all the compounds studied (figure 3). Line widths are sensitive to the solvent used, DMF giving the best resolution (figure 3a). The spectrum of the red $Mn_2O_2(phen)_3(DMF)_2 (PF_6)_3$ in DMF is identical to that obtained by dissolving the green parent complex in the same solvent. Again, both the red and green complexes gave identical spectra in acetonitrile. Similar observations were also made for the pyridine-substituted complexes. We conclude that the mixed ligand complexes have very different IVTA characteristics, but nearly identical EPR parameters.

3.3 *Interpretation of the EPR spectra*

For an antiferromagnetically coupled binuclear system with unpaired electrons, the
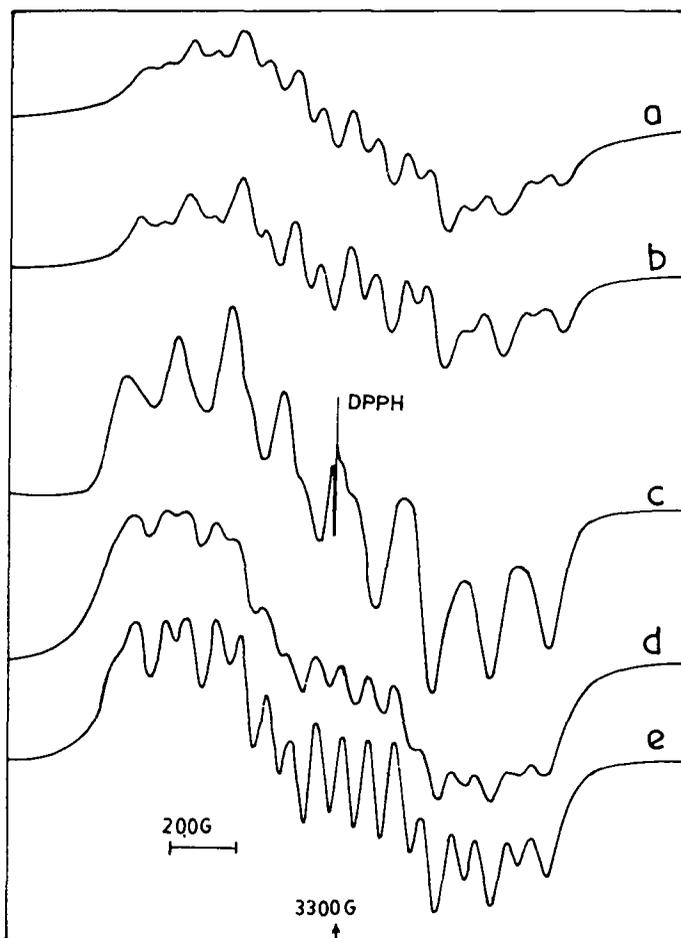
Figure 2. X-band EPR spectra $(\nu = 9{\cdot}228\,\text{GHz}, \quad T = 120\,\text{K})$, of polycrystalline samples of (a) $[\text{Mn}_2\text{O}_2(4,4'\text{-dmbp})_4](\text{PF}_6)_3$, (b) $[\text{Mn}_2\text{O}_2(5,5'\text{-dmbp})_4](\text{PF}_6)_3$, and (c) $\text{Mn}_2\text{O}_2(\text{phen})_4(\text{PF}_6)_3$, (d) and (e) are computer simulations with isotropic widths of 65 G and 50 G, respectively.

total spin Hamiltonian may be expressed as the sum of the single ion Hamiltonians, $\mathscr{H}_1$ and $\mathscr{H}_2$ and the interaction term $\mathscr{H}_{12}$, assuming the orbital angular momentum to be completely quenched. The isotropic Heisenberg Hamiltonian $\mathscr{H}_{12} = -2J\text{S}_1\cdot\text{S}_2$ describes the spin–spin coupling and it is the largest term in the combined spin Hamiltonian. Therefore, the $\text{Mn(III)}(S_1 = 2)$–$\text{Mn(IV)}(S_2 = 3/2)$ system will have a doublet ground state well-removed from the other states. The following treatment is strictly valid only when the magnitude of the exchange parameter, J, is much greater than the zero-field splitting parameter, D. This condition is satisfied for the Mn(III, IV) complexes which have $|J| \gtrsim 100\,\text{cm}^{-1}$ (Goodwin and Sylva 1967).

The spin-Hamiltonian for any state, S can be written in the coupled regimes as follows:

$$\mathscr{H}_{\text{coupled}} = \text{H}\cdot g\cdot\text{S} + \text{S}\cdot A_1\cdot\text{I}_1 + \text{S}\cdot A_2\cdot\text{I}_2, \tag{1}$$

$$\mathscr{H}_{\text{uncoupled}} = \text{H}\cdot g_1\cdot\text{S} + \text{H}\cdot g_2\cdot\text{S} + \text{S}\cdot A_1'\cdot\text{I}_1 + \text{S}\cdot A_2'\cdot\text{I}_2. \tag{2}$$

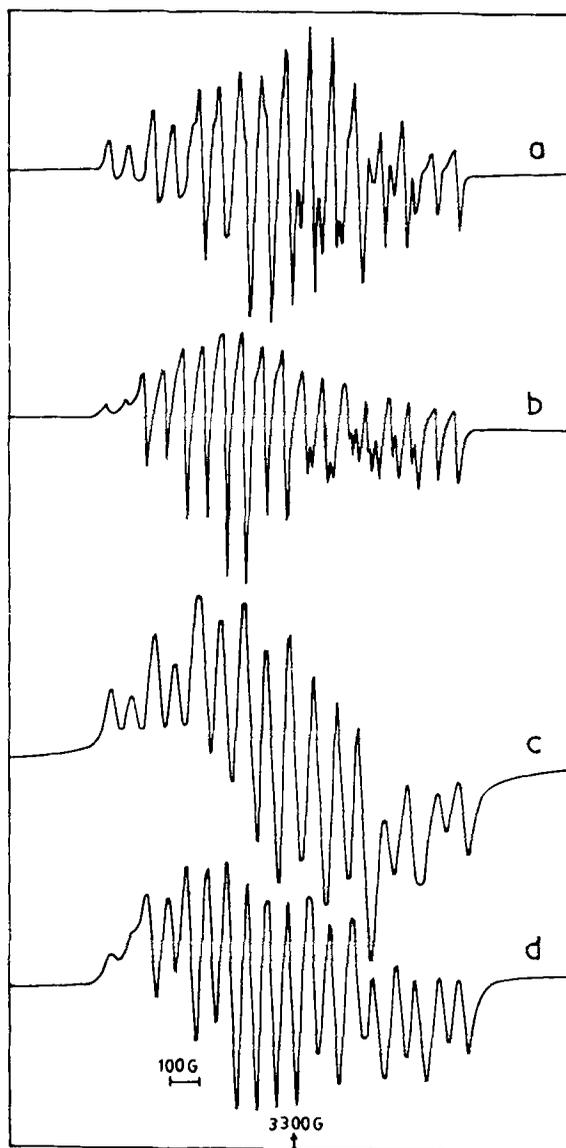**Figure 3.** Two typical frozen solution EPR spectra at X-band ($v = 9.198$ GHz, $T = 120$ K), (a) $[Mn_2O_2(phen)_4](PF_6)_3$ in DMF, and (c) $[Mn_2O_2(bpy)_4](PF_6)_3$ in acetonitrile, (b) and (d) are computer simulations with isotropic widths of 25 G and 11 G, respectively.

The coupled tensors g, A_1 and A_2 can be related to those of the non-interacting ions via projection of S_1 and S_2 on S, and can be written as,

$$g = \alpha g_1 + \beta g_2, \tag{3}$$

$$A_1 = \alpha A'_1, \tag{4}$$

$$A_2 = \beta A'_2, \tag{5}$$

where,

$$\alpha = \{S(S+1) + S_1(S_1+1) - S_2(S_2+1)\}/\{2S(S+1)\}, \tag{6}$$

and

$$\beta = \{S(S+1) + S_2(S_2+1) - S_1(S_1+1)\}/\{2S(S+1)\}. \tag{7}$$

The quantities α and β for the various spin-states are as follows:

S	α	β
1/2	2	-1
3/2	4/5	1/5
5/2	22/35	13/35
7/2	4/7	3/7

Whenever the condition $|J| \gg |D|$ is not satisfied, S is no more a good quantum number and the above equations will have to be modified. A treatment including the zero-field parameter has been given by Euler (1986) for the cases $S_1 = \frac{1}{2}$ and $S_2 = 1$, 3/2, 2 and 5/2.

Coming to the individual ion parameters, in a distorted octahedral environment, the orbital singlet ground state of Mn^{3+} [$^5B_2$ in $C_{2v}(x)$notation] will be coupled to the components of the excited T_2 state via spin-orbit interaction. To first order, the g-values can be written as

$$g_{\|} = g_e - 8\lambda/\Delta, \tag{8}$$

$$g_{\perp} = g_e - 2\lambda/\Delta, \tag{9}$$

where, $g_e = 2\cdot0023$ is the free-spin value, λ is the one-electron spin-orbit coupling constant for Mn^{3+} and Δ is the energy of the excited state (with splitting neglected) with respect to the ground state. The free ion value for λ is $360\,cm^{-1}$ and the g-values are predicted to be less than $2\cdot00$. The hyperfine splitting is expected to contain appreciable dipolar contribution. However, data on the Mn^{3+} ion is scarce. In TiO_2 the principal values range from $0\cdot0053$ to $0\cdot0085\,cm^{-1}$ (Goodman and Raynor 1970).

For the Mn^{4+} site the ground orbital singlet [$^4B_2$ in $C_{2v}(x)$] is coupled to the components of the excited T_2, but not T_1. In this case the g-values can be written as

$$g_{\|} = g_e - 8\lambda/\Delta_0, \tag{10}$$

$$g_{\perp} = g_e - 8\lambda/\Delta_1, \tag{11}$$

where, Δ_0 and Δ_1 are the energies of the two components of $T_2(^4B_2$ and ^4E, with the splitting of the latter neglected). The spin-orbit parameter, λ is expected to be slightly larger in this case ($\sim 390\,cm^{-1}$) and again the g-values are predicted to be less than $2\cdot00$. The hyperfine splitting is almost entirely due to core-polarisation which produces a field of $\sim -192\,kG$ at the nucleus with a small orbital contribution of -4 to $-6\,kG$. The A-tensor is therefore expected to be almost isotropic. The parameters in Al_2O_3 are $0\cdot00696\,cm^{-1}$ ($A_{\|}$) and $0\cdot00704\,cm^{-1}$ ($A_{\perp}$) (Abragam and Bleaney 1970).

For the Mn(III, IV) complexes, hyperfine coupling with the two ^{55}Mn nuclei ($I = 5/2$) produces a multiline EPR spectrum. The number of lines expected depends on the extent of delocalisation of the odd electron and three different cases can be

considered: (a) complete delocalisation – equal hyperfine coupling with the two nuclei results in a set of 11 lines with intensity ratio 1:2:3:4:5:6:5:4:3:2:1. The pattern is not expected to be temperature-dependent. (b) Localised case – maximum of $6 \times 6 = 36$ lines are expected. For the ground ($S = \frac{1}{2}$) state, we have, $A_1 = 2A_1'$ and $A_2 = -A_2'$. Since $A_1' \sim A_2'$, we have the special case $A_1 = 2A_2$ which gives rise to a 16-line pattern with intensity ratio 1:1:2:2:3:3:3:3:3:3:3:3:2:2:1:1. This is the usual spectrum observed for many Mn(III, IV) complexes in frozen solutions. (c) Localised with fast exchanging (hopping) between the two centres – here again 11 lines are expected as in (a), but the spacing between them can be related to A_1' and A_2' of the individual ions Mn^{3+} and Mn^{4+}, as

$$A = (A_1 + A_2)/2 = (2A_1' - A_2')/2. \tag{12}$$

The spectrum is expected to be temperature-dependent. Averaging to give 11 lines results when the rate of exchange is much faster than $|A_1| - |A_2|$, where A_1 and A_2 are expressed in hertz. With rates close to this critical rate, broadening of the individual lines are observed and much below the critical rate the spectrum is the same as for (b).

The line widths observed for powder samples have several contributions, viz., (i) spin dipolar interaction, (ii) spin exchange between different molecules in the lattice, (iii) thermal population of excited states, and (iv) electron exchange between the two centres. Of these, (i) and (ii) are intermolecular processes present in magnetically concentrated systems, while (iii) and (iv) are intramolecular processes peculiar to mixed-valent antiferromagnetically coupled dinuclear systems. While dipolar interaction is expected to broaden all the hyperfine lines resulting in a broad envelope, intermolecular exchange in the fast limit is expected to give a single narrow line. Population of thermally accessible excited states increases the number of transitions and may eventually contribute to broadening. Intramolecular electron transfer leads to a line broadening and in the fast limit gives a set of 11 lines. Since the two hyperfine couplings are opposite in sign, the broadening is predicted to set in on the outer lines and thereby reduce the spread of the spectrum as the transfer rate increases.

In most cases reported here, exchange narrowed lines were obtained with peak to peak width ranging from 300 to 750 G. In the case of $[Mn_2O_2(bpy)_3(py)_2](ClO_4)_3$ and $[Mn_2O_2(phen)_3(py)_2](ClO_4)_3$ dipolar broadened lines having a width of 1300 G were observed. The PF_6^- salts of $[Mn_2O_2(phen)_4]^{3+}$, $[Mn_2O_2(bpy)_4]^{3+}$, $[Mn_2O_2(5,5'-dmbp)_4]^{3+}$ and $[Mn_2O_2(4,4'-dmbp)_4]^{3+}$ as well as $[Mn_2O_2(bpy)_3phen](ClO_4)_3$ show resolution of the hyperfine splitting to varying extents (figure 2). We have attempted to simulate these spectra assuming an isotropic line width of 65 G (figure 2d). Quantitative fitting is not expected here because the dipolar effects are not included in the simulation. The calculated spectrum for a width of 50 G is also included and it shows further splittings towards an eventual resolution of 16 lines (compare figures 2a and 2c). The line narrowing observed upon cooling the samples is most likely due to reduction in intensity of the signal from excited spin states as well as a relaxation effect. In no case did we observe a narrowing effect with reduction in hyperfine spacing. Since the difference between $|A_1|$ and $|A_2|$ is $0.0070 \, cm^{-1}$, we conclude that the electron transfer rate in the solid samples is much less than $2 \times 10^8 \, Hz$.

In frozen solutions 16 lines ($A_1 \sim 2A_2$) are readily seen in all cases while in some cases mostly for DMF solutions, further splittings are resolved (figure 3). Two typical simulations are also shown (figures 3b, d). The previous computer simulations (Cooper *et al* 1978; Dismukes and Siderer 1981) were done assuming isotropic g and A

Table 1. Spin-Hamiltonian parameters.

	$g_\parallel$	$g_\perp$	$A_{\parallel 1}^*$	$A_{\perp 1}^*$	$A_{\parallel 2}^*$	$A_{\perp 2}^*$
$[Mn_2O_2(phen)_4](PF_6)_3$ (polycrystalline)	2·06	1·98	14	14	7	7
$[Mn_2O_2(bpy)_4](ClO_4)_3$ (in acetonitrile)	2·071	1·952	13·7	13·1	6·9	6·6
$[Mn_2O_2(phen)_4](PF_6)_3$ (in DMF)	2·078	1·962	13·8	13·0	6·9	6·5

$^*10^{-3} cm^{-1}$

values. Cooper *et al* (1978) did try to artificially 'simulate' the anisotropy by using an M_I-dependent line width with an isotropic Hamiltonian. However, this procedure has theoretical justification only for a fluid solution. Our spectra which were fit to the axial Hamiltonian show that significant anisotropy is present in these compounds. The fitting is not exact due to the constraints in the model viz., isotropic line width, treatment of one of the ^{55}Mn coupling (A_2) only to first order and also neglect of the small amount of Mn^{2+} impurity and the contribution from the excited spin states. The parameters derived by simulation are summarised in table 1.

The striking feature of the spectra of the various compounds is that they correspond to almost identical g and A values. The parameters in solution and solid, wherever resolution was possible, are also very similar. The major contribution to hyperfine splitting arises from core-polarisation. Covalent delocalisation is expected to reduce the A values. Since the t_{2g} electrons are not delocalised to any great extent, the A values are not very sensitive to the type of ligands. The complex with porphyrin does show a reduced coupling constant which may be attributed to increased covalency (Camenzind *et al* 1983). The g-anisotropy is also very small in these compounds due to the small ($\lambda/\Delta \approx 0·02$ for Mn^{3+} and $\approx 0·013$ for Mn^{4+}) contribution from spin-orbit interaction. From the first order equations g-shifts of nearly 0·1 are expected for Mn^{3+} (g_1). The actual shift is found to be less than this value showing that first-order interpretation using a single free-ion λ is not sufficient to account for the small variation of g from free-spin value.

Finally, it may be mentioned that recently Nishida (1988) has reported a multiline spectrum very similar to that of the Mn(III, IV) complex and attributed the same to an Mn(III, III) complex with very small antiferromagnetic coupling ($J \approx -0·88 cm^{-1}$), without a detailed interpretation of the spectrum. This assignment is in error because exchange between identical spins ($S_1 = S_2 = 2$) should give rise to an 11-line pattern with hyperfine splitting equal to half that of the individual centres. The 16-line pattern with a spacing of 77 G is not compatible with this description. The author has not considered a possible disproportionation of Mn(III) with eventual formation of the Mn(III, IV) complex in solution, and also has not reported solution magnetic susceptibility data. We tend to maintain that the multiline spectra of the type shown here for solid and frozen solution samples are typical for dinuclear Mn(III, IV) complexes and that the spectral parameters are not very sensitive to the coordination environment of the manganese ions.

3.4 *Mn(III, IV) complexes as catalysts for water oxidation*

Several years ago, Calvin (1974) reported that the bpy complex oxidises water photolytically, which claim was subsequently withdrawn (Cooper and Calvin 1974).

Recently Ramaraj *et al* (1986) have reported oxygen evolution in a heterogeneous system containing solid $[Mn_2O_2L_4](ClO_4)_3 L = bpy$, phen, in contact with an aqueous solution of $(NH_4)_2 Ce(NO_3)_6$. We could reproduce this experiment and obtain similar results also with the py- and DMF-substituted complexes. Gas bubbles were seen to evolve from the surface of the undissolved portion of the complexes added to a 40% aqueous solution of $(NH_4)_2 Ce(NO_3)_6$. In the absence of the solid phase no gas evolution occurred. Also no gas evolved in the absence of the ceric salt.
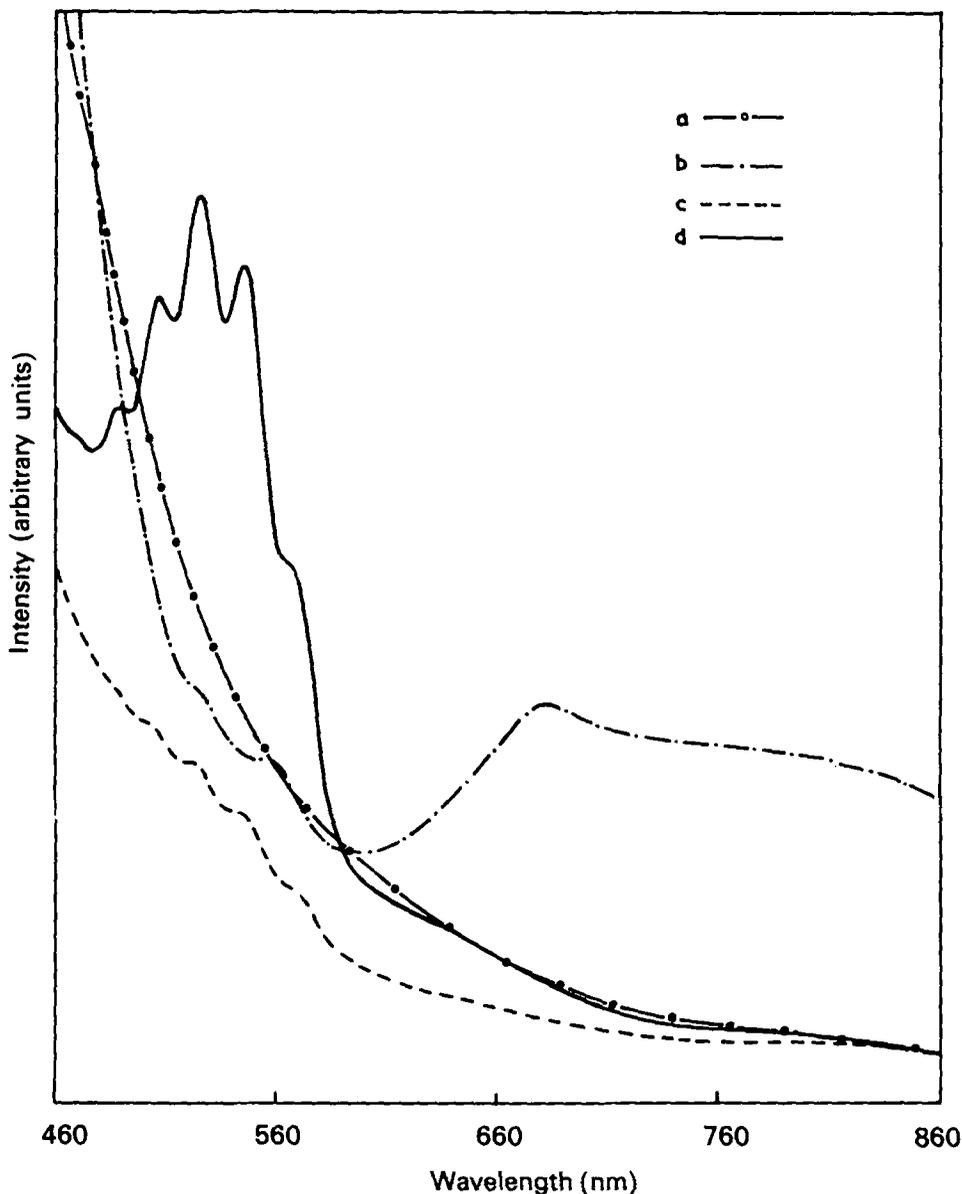

Figure 4. Visible absorption spectra of aqueous solutions of $[Mn_2O_2(bpy)_4](ClO_4)_3$: (a) at neutral pH, (b) at pH 4·5, (c) in the presence of Ce^{4+}, and (d) after aging solution (e) for a day.

The volume of the gas evolved was measured using a gas burette and was confirmed to be oxygen by its quantitative absorption by alkaline pyragallol. Gas evolution could be observed for 20–30 h after which time it became imperceptibly slow. While detailed kinetic studies are not at present available and the rates are also expected to be sensitive to the grain size in the solid phase, a turnover number (defined as the number of moles of O_2 evolved per four moles of the complex) greater than 1 in all cases studied indicate that the process is catalytic.

The electronic spectrum of the bpy complex in water in presence of $(NH_4)_2 Ce(NO_3)_6$ is shown in figure 4. It has at least six bands in the region 17·8 to 20·8 kK and the IVTA band is almost completely absent. This means that the solution contains only mononuclear species. The intensity of the higher energy bands slowly increases with time. This band can be assigned to the permanganate ion (Lever 1984). The formation of this ion in the oxygen-evolving solution complicates the picture because MnO_4^- in acidic medium can also oxidise water slowly. However, this alone can not account for the copious evolution of oxygen bubbles from the solid complex in heterogeneous solution.

4. Conclusions

The position and intensity of the IVTA band in Mn(III, IV) complexes is very sensitive to the solvent because, even weakly coordinating solvents can perturb the coordination sphere of the labile Mn(III) site. Partially substituted complexes could be prepared by crystallising the parent symmetrical complexes from solvents like DMF and pyridine. These have very different visible spectra but virtually identical EPR spectra. Resolution of the hyperfine lines in polycrystalline samples is possible for some PF_6^- salts and they have parameters similar to that observed in frozen solutions. While the properties of the IVTA band are controlled mainly by the composition of the outermost molecular orbitals, these orbitals affect the EPR g and A values of Mn^{3+} and Mn^{4+} only marginally, the reason being the dominance of the core-polarisation contribution to A and the rather small spin-orbit interaction. Regarding the catalytic role of these complexes for oxidation of water in the presence of Ce^{4+}, while it is clear that oxygen evolution takes place at the catalyst/water interphase, the picture is complicated by the formation of MnO_4^-.

References

Abragam A and Bleaney B 1970 *Electron paramagnetic resonance of transition ions* (Oxford: Clarendon)
Biggins J (ed) 1987 *Progress in photosynthetic research* (Dordrecht: Martinus Nijhoff) vol. 1
Calvin M 1974 *Science* **184** 375
Camenzind M J, Hollander F J and Hill C L 1983 *Inorg. Chem.* **22** 3776
Cooper S R and Calvin M 1974 *Science* **185** 376

Cooper S R and Calvin M 1977 *J. Am. Chem. Soc.* **99** 6623

Cooper S R, Dismukes G C, Klein M P and Calvin M 1978 *J. Am. Chem. Soc.* **100** 7248

Dismukes G C and Siderer Y 1981 *Proc. Natl. Acad. Sci. USA* **78** 274

Euler W B 1986 *Inorg. Chem.* **25** 1871

Furniss B S, Hannaford A J, Rogers V, Smith P W G and Tatchell A R (eds) 1978 *Vogel's text book of practical organic chemistry* (London: ELBS)

Goodman B A and Raynor J B 1970 *Adv. Inorg. Chem. Radiochem.* **13** 136

Goodwin H A and Sylva R A 1967 *Aust. J. Chem.* **20** 629

Hush N S 1967 *Prog. Inorg. Chem.* **8** 391

Inoue M 1978 *Bull. Chem. Soc. Jpn.* **51** 1400

Kambara T and Govindjee 1985 *Proc. Natl. Acad. Sci. USA* **82** 6119

Lever A B P 1984 *Inorganic electronic spectroscopy* (New York: Elsevier)

Morrison M M and Sawyer D T 1978 *Inorg. Chem.* **17** 333, 338

Mulay M and Padhye S 1987 *Proc. Indian Natl. Sci. Acad.* **B53** 471

Nishida Y 1988 *Inorg. Chim. Acta* **151(B22)** 177

Nyholm R S and Turco A 1960 *Chem. Ind. (London)* 74

Paula J C and Brudvig G W 1985 *J. Am. Chem. Soc.* **107** 2643

Plaksin P M, Stoufer R C, Mathew M and Palenik G J 1972 *J. Am. Chem. Soc.* **94** 2121

Rajasekharan M V and Manoharan P T 1981 *Mol. Phys.* **44** 1145

Ramaraj R, Kira A and Kaneko M 1986 *Angew. Chem., Int. Ed. Engl.* **25** 825

Sasse W H F and Whittle C P 1961 *J. Chem. Soc.* 1347

Stebler M, Ludi A and Bürgi H B 1986 *Inorg. Chem.* **25** 4473